Quantum Electronics

Russian Academy of Sciences Turpion

Lasing characteristic of new Russian laser ceramics

To cite this article: V.V. Bezotosnyi *et al* 2018 *Quantum Electron.* **48** 802

View the article online for updates and enhancements.

You may also like

- 16.7 W 885 nm diode-side-pumped actively *Q*-switched Nd:YAG/YVO_4 intracavity Raman laser at 1176 nm
Pengbo Jiang, Guizhong Zhang, Jian Liu et al.
- Numerical study on the selective excitation of Helmholtz–Gauss beams in end-pumped solid-state digital lasers with the control of the laser gain transverse position provided by off-axis end pumping
Ko-Fan Tsai and Shu-Chun Chu
- Analysis of pump excited state absorption and its impact on laser efficiency
W R Kerridge-Johns and M J Damzen

This content was downloaded from IP address 18.116.12.230 on 21/05/2024 at 19:20

 ©2018 Kvantovaya Elektronika and Turpion Ltd

LASERS

https://doi.org/10.1070/QEL16756

Lasing characteristic of new Russian laser ceramics

V.V. Bezotosnyi, V.V. Balashov, V.D. Bulaev, A.A. Kaminskii, A.Yu. Kanaev, V.B. Kravchenko, A.V. Kiselev, Yu.L. Kopylov, A.L. Koromyslov, O.N. Krokhin, K.V. Lopukhin, S.L. Lysenko, M.A. Pankov, K.A. Polevov, Yu.M. Popov, E.A. Cheshev, I.M. Tupitsyn

Abstract. **Lasing efficiency of neodymium-doped yttrium–aluminium garnet (YAG) ceramic samples, which were fabricated at the Fryazino Branch of the Kotelnikov Institute of Radio Engineering and Electronics, Russian Academy of Sciences and the SLPG 'Raduga' in 2016–2017, is studied under the conditions of end- and side-pumping. The efficiency of lasers based on this ceramics was 64% in the case of end-pumping and 68%–70% upon side-pumping. The laser level lifetimes are measured in ceramics with neodymium concentrations of 1, 2, 3, and 4 at%. The measured lifetimes well agree with the literature data. The dependences of the lasing threshold on the cavity length under the conditions of transverse mode locking and diode end-pumping are studied for different samples of laser ceramics in a semiconfocal cavity. In sum, the performed investigations showed that the quality of the first industrial samples of Russian laser ceramics are highly competitive in quality with the ceramics produced by Konoshima Chem. Corp., Ltd., which is considered by the laser community as an etalon.**

Keywords: *laser ceramics, sintering aids, transverse mode locking.*

1. Introduction

One of the technological problems in obtaining high-quality optical ceramics, in particular, yttrium–aluminium garnet (YAG) ceramics of laser quality, is the problem of eliminating residual pores. The appearance of residual porosity in the process of solid-phase reactive sintering is caused by several factors, including the morphology and dispersivity of starting oxide powders [1–4], deviation from stoichiometry in the chemical composition of the oxide mixture [5], compaction and sintering conditions [6–10], and the existence and type of sintering additives (SAs) [11–16]. Combinations of SAs at which the concentration of residual pores does not exceed 0.0002% [17] were found at the Fryazino Branch of the Kotelnikov Institute of Radio Engineering and Electronics, Russian Academy of Sciences (FIRE) [17]. Yttrium and neodymium powders (Lanhit Ltd.) and aluminium oxide powders (Sumitomo Chem. Co., Ltd) were used as starting materials under laboratory and industrial conditions. Hereinafter, all materials and samples produced at FIRE, SPLG 'Raduga', and Konoshima Chem. Co., Ltd are denoted by F, R, and K, respectively.

The powders of rare-earth oxides were preliminarily chemically reprecipitated by a traditional method [7] to eliminate hard agglomerates. Aluminium oxide powders were used without preliminary treatment. The oxide powders taken in the stoichiometric proportion $Y_{3-x}Nd_xAl_5O_{12}$ (x = 0.001, 0.002, 0.003, and 0.004) were mixed in a planetary mill using isopropanol as a dispersive medium. Then, the mixture was granulated in a spray dryer to obtain press-powder. The use of granulated press powder is an extremely important technological feature for obtaining a minimal residual porosity of ceramics. Ideal spheres of this press powder ensure maximally homogeneous packing density of compacted particles. Figure 1 shows a photograph of the press powder and the microstructure of ceramics without residual pores.

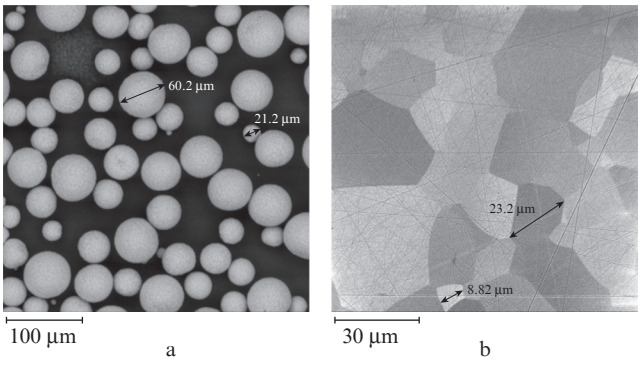

Figure 1. (a) Microphotograph of press powder obtained by spray drying and (b) ceramics microstructure.

The press powder with granules 50–70 μm in diameter was preliminarily compacted to desired dimensions by uniaxial pressing at a pressure of 20–50 MPa and finally compacted in an isostatic press at a pressure of 250 MPa. The compacts were sintered in a vacuum furnace with a tungsten heater at a temperature of 1600–1780 °C. After sintering, the samples were annealed in air at a temperature of 1100–1450 °C.

V.V. Bezotosnyi, A.L. Koromyslov, O.N. Krokhin, K.A. Polevov, Yu.M. Popov, E.A. Cheshev, I.M. Tupitsyn P.N. Lebedev Physical Institute, Russian Academy of Sciences, Leninsky prosp. 53, 119991 Moscow, Russia; e-mail: imtupitsyn@yandex.ru;
V.V. Balashov, V.B. Kravchenko, Yu.L. Kopylov, K.V. Lopukhin Kotelnikov Institute of Radio Engineering and Electronics (Fryazino Branch), Russian Academy of Sciences, pl. Akad. Vvedenskogo 1, 141190 Fryazino, Moscow region, Russia;
V.D. Bulaev, A.Yu. Kanaev, A.V. Kiselev, S.L. Lysenko, M.A. Pankov SLPG 'Raduga', fse, PO box 771, 600910 Radyzhnyi, Vladimir region, Russia;
A.A. Kaminskii Federal Scientific Research Centre 'Crystallography and Photonics', Russian Academy of Sciences, Leninsky prosp. 59, 119333 Moscow, Russia

Received 13 June 2018; revision received 1 August 2018
Kvantovaya Elektronika **48** (9) 802–806 (2018)
Translated by M.N. Basieva

The aim of the present work is to estimate the lasing characteristics of ceramic samples and to use a laser method for express-estimation of laser ceramics porosity.

2. Lasing efficiency of new Nd:YAG ceramics

We studied samples of Nd^{3+}:YAG ceramics with a neodymium concentration of 1 at%. Samples R had dimensions of 3×3×4, 3×3×11, and 4.5×5×20 mm, while dimensions of sample F were ∅12×5 mm. Etalon ceramic samples K were 10×10×3.3 mm in size. Photographs of the ceramic samples are presented in Fig. 2.

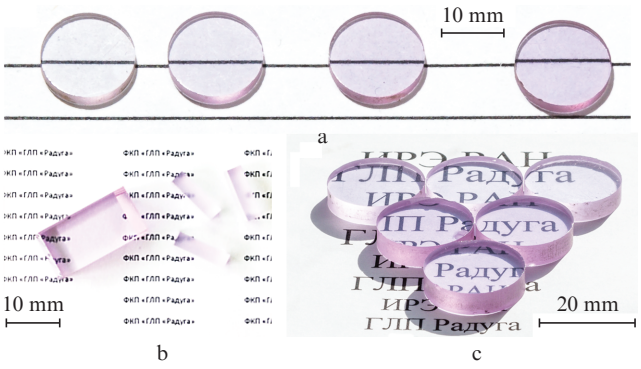

Figure 2. Photographs of ceramic samples (a) F and (b, c) R.

The lasing characteristics of new ceramics were studied in laser schemes with diode end- and side-pumping. The laser scheme with diode end-pumping is shown in Fig. 3. The laser cavity was formed by spherical mirror M1 and plane output mirror M2, which allowed us to avoid intracavity astigmatism [18]. Spherical mirror M1 was highly reflecting at the lasing wavelength (R_{1064} = 99.96%) and transparent at the pump wavelength ($T_{808} \geqslant 99\%$). In the experiments, we used mirrors M1 with radii of curvature of 150 and 200 mm. The reflectivity of plane mirror M2 at the lasing wavelength was 96%. The faces of the active elements were antireflection coated for the lasing and pump wavelengths. The lasing efficiency was measured in a cavity configuration close to semiconfocal.

Pumping was performed by a laser diode (LD) with an output power up to 10 W and a wavelength of 808 nm. To decrease the influence of thermooptical distortions of the active medium, we used repetitively pulsed pumping with an off-duty ratio of 20. The lasing efficiency was measured with an off-duty ratio of 2, which allowed measuring the average power with a sufficient accuracy. The FWHM diameter of the laser beam in the active element was 220 μm. The pump wavelength was tuned to 808 nm by controlling the LD temperature, for which the LD was mounted on a thermoelectric Peltier-effect module.

The lasing threshold was recorded using a Thorlabs BC C106-VIS CCD camera (wavelength range 350–1100 nm). A K8 glass plate reflected a part of the output radiation to reduce the intensity of radiation incident on the CCD matrix. An IKS-7 filter placed in front of the CCD camera was used to suppress the residual pump radiation.

The scheme of a laser with diode side-pumping is shown in Fig. 4. The laser cavity in this case is formed by two plane mirrors, one of which was highly reflecting at the lasing wavelength, and the reflectivity of the second mirror was R = 70%.

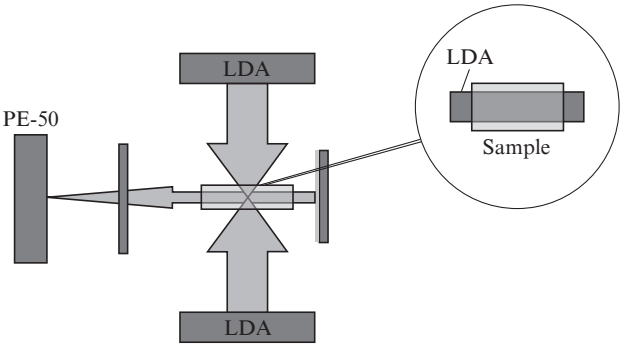

Figure 4. Principal scheme for measuring the laser ceramics efficiency upon side-pumping by an LD array (LDA).

The pump and lasing energies were measured with a PE-50 calorimetric energy meter. The powers of the pump and laser pulses were calculated by the measured energies taking into account the recorded pulse shape (Fig. 5). The pulsed laser power was determined after its stabilization at the end of the pump pulse. Pumping was performed by diode arrays (Inject Ltd.) through two side surfaces of the active ceramic element.

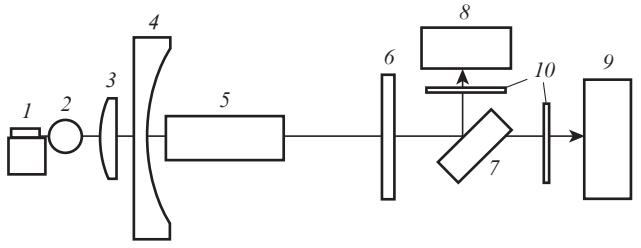

Figure 3. Scheme of the laser setup with diode end-pumping: (*1*) laser diode; (*2*, *3*) elements for pump beam collimation; (*4*, *6*) cavity mirrors M1 and M2, respectively; (*5*) active Nd:YAG ceramic element; (*7*) etalon plate–attenuator; (*8*) CCD camera; (*9*) calorimetric detector; (*10*) colour light filters.

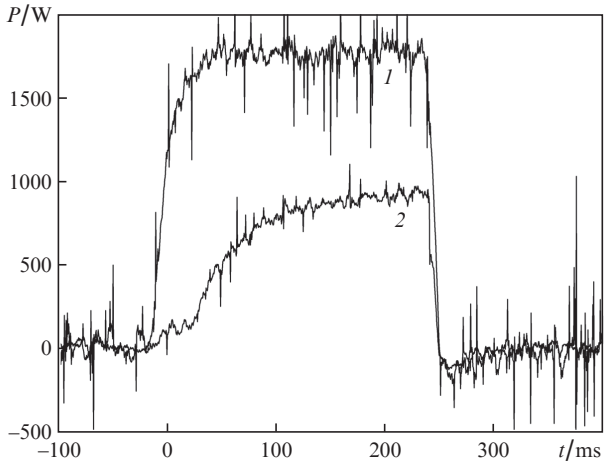

Figure 5. Temporal shapes of (*1*) pump and (*2*) laser pulses under side-pumping by LD arrays.

The pump pulse duration was 250 μs, and the pulse repetition rate was 1 Hz.

The lasing efficiencies of samples R and K in the scheme with diode end-pumping are compared in Fig. 6. The slope efficiencies η_{lp} were measured to be 64% for ceramics R and 65% for samples K.

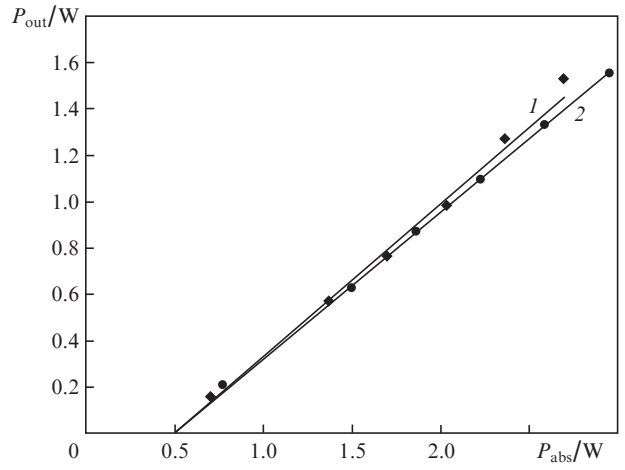

Figure 6. Comparison of slope efficiencies of (*1*) etalon ceramics K and (*2*) ceramic sample R 3×3×4 mm in size upon end-pumping.

The measured lasing characteristics of ceramics R in the scheme with side-pumping are presented in Fig. 7. The slope efficiency was 69%–70%. The higher efficiency in this case is explained by uniform pumping of the active ceramic elements under the conditions of two-side-pumping. It should be noted that the mentioned efficiency of ceramic samples R was obtained at a pump power up to 1.8 kW. In this case, the pulsed power of laser radiation was 900 W.

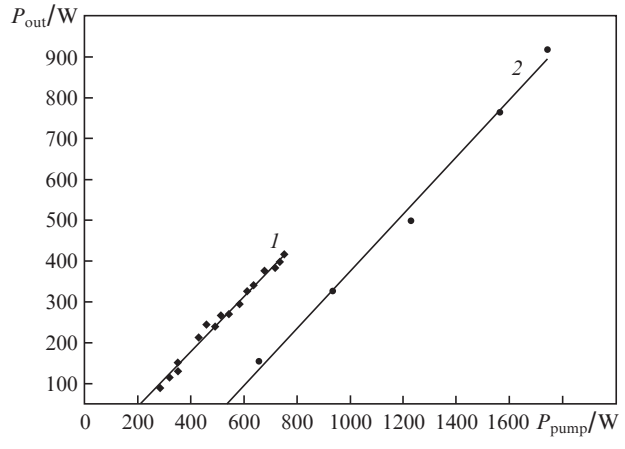

Figure 7. Slope efficiency of ceramic samples R with dimensions of (*1*) 3×3×11 mm (η_{tp} = 68%, P_{th} = 136 W) and (*2*) 4.5×5×20 mm (η_{tp} = 70%, P_{th} = 462 W) upon diode side-pumping.

3. Laser level lifetimes in Nd:YAG ceramics with different neodymium concentrations

The laser level lifetime was measured in Nd:YAG ceramic samples F 6 mm in diameter and 1 mm thick with dopant concentrations of 1, 2, 3, and 4 at%. The lifetimes were measured by luminescence kinetics upon excitation by 250-μs LD pulses with an off-duty ratio of 40. The pump radiation was collimated to a diameter of about 1 mm into the studied ceramic samples. The luminescence kinetic was recorded using an InGaAS photodetector with a bandwidth of 5 GHz and a Tektronix TDS 2012C oscilloscope with a bandwidth of 100 MHz. The measured luminescence decay curves for aforementioned ceramic samples are shown in Fig. 8.

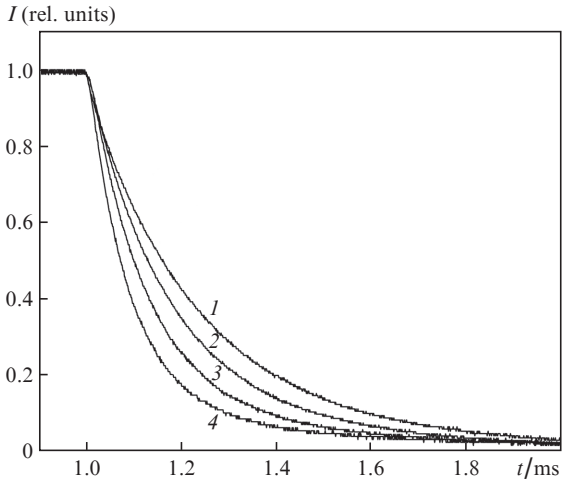

Figure 8. Luminescence kinetics of ceramic samples F with Nd^{3+} concentrations of (*1*) 1, (*2*) 2, (*3*) 3, and (*4*) 4 at%.

The measured laser level lifetimes for Nd:YAG ceramics F and (for comparison) the corresponding lifetimes for ceramics K taken from [19] are listed in Table 1. One can see that the laser level lifetimes for ceramic samples F with different neodymium concentrations well agree with the corresponding literature data for ceramics K.

Table 1. Laser level lifetime for Nd:YAG ceramics F and K.

Concentration Nd^{3+} (at%)	Lifetime/μs	
	Ceramics F	Ceramics K
1	243	234
2	200	174
3	136	–
4	105	94

4. Method of express estimation of laser ceramics porosity

It was shown in [20] that the residual porosity of laser ceramics considerably decreases the output power and efficiency of lasers with ceramic active elements. This is mainly caused by scattering of light by residual pores with dimensions comparable with the laser wavelength. Ceramics can be called high-quality ceramics if the volume concentration of residual pores in it is about 0.0001%, because it is this concentration at which residual pores almost do not affect the laser efficiency. Thus, it is important to find an efficient method for estimating low concentrations of residual pores. In our experiments, we measured the lasing threshold, which, as was found, is rather sensitive to low losses related to scattering in porous ceramics [17].

The lasing threshold was measured in the scheme with end-pumping in the range of cavity configurations that, under the conditions of transverse mode locking, exhibit high sensitivity to losses related to any phase distortions changing the ensemble of modes in the fundamental mode structure and caused, for example, by scattering in the active medium [21]. To measure the dependence of the lasing threshold on the cavity length in the range of semiconfocal configuration upon transverse mode locking, we used the laser scheme with end-pumping (see Fig. 3). Output mirror M2 was mounted on a translation stage (Standa), which allowed us to change the cavity length with an accuracy of 2.5 μm almost in the entire range of its stability without misalignment. The optical system formed in the active element a pump beam with a diameter of 220 μm, which is twofold smaller than the size of the Gaussian cavity mode. This satisfied the transverse mode locking condition [22] in the cavity configurations described by the expression

$$\arccos\sqrt{g_1 g_2} = \pi\frac{r}{s},$$

where r/s characterises the degeneration, $g_{1,2} = 1 - L/R_{1,2}$ is the cavity stability parameter, L is the cavity length, and $R_{1,2}$ are the radii of curvature of mirrors [22]. The lasing thresholds of the ceramic samples were experimentally measured in the cavity configuration close to semiconfocal, i.e., with $r/s = 1/4$ and $L = 76$ mm for a mirror with $R_1 = 150$ mm. Transmittance T of the plane output mirror was 4%. The measured dependences of the lasing threshold on the deviation from cavity length L corresponding to the confocal cavity configuration for Nd:YAG (1 at%) ceramic samples F, R, and K are presented in Fig. 9. One can see that the dependences of lasing threshold P_{th} on detuning ΔL for all three types of ceramics differ by no more than 4 mW. Since the lasing thresholds for lasers based on Nd:YAG ceramics with concentrations of residual pores of 60, 20, and 1 ppm are 1.6 W, 0.7 W, and 12 mW, respectively [21], the slope of the threshold dependence on the pore concentration was estimated by the linear regression method to be 26 mW ppm^{-1}. The root-mean-square deviation within the given porosity range is lower than 10%. Therefore, the porosity of the studied ceramic samples differ by no more than 0.0001% from the porosity of etalon ceramics K with a pore concentration of 1 ppm, which testifies to a high quality of ceramics of the mentioned manufacturers.

We also studied the homogeneity of ceramic samples R with dimensions of 3×3×4 and 3×3×6 mm cut from different regions of a ceramic disk 70 mm in diameter (Fig. 9b).

Dependences $P_{th}(\Delta L)$ were measured in the repetitively pulsed regime with pulse duration $\tau = 1$ ms and period $T = 20$ ms. The laser diode working temperature provided a pump wavelength of 808.5 nm, which coincided with the absorption peak of the active element. The width of the pump radiation spectrum was 1.2 nm at the LD current up to 4 A. The samples with dimensions of 3×3×4 and 3×3×6 mm absorbed 80±1% and 99±1% of the pump power, respectively.

All measurements were performed at constant working parameters of the optical pumping system, which provided a fixed pump beam diameter in the active element. In experiment, the cavity was aligned to achieve the minimal lasing threshold and a required spatial distribution of the laser beam intensity upon transverse mode locking in the semiconfocal configuration. The lasing thresholds determined at cavity length $L = 71$ mm (which corresponded to a 5-mm deviation from the semiconfocal configuration (76 mm)) for ceramic samples R varied from 4 to 7 mW (this corresponds to residual porosity of 0.1 ppm), which testifies to a high homogeneity of the laser ceramics.

5. Conclusions

Our study of the lasing characteristics of Russian ceramics R and F showed high (up to 70%) slope efficiency η_{dif} of pump radiation conversion to laser radiation, while the maximum possible efficiency for this type of ceramics is $\eta = 72\%$ (76% due to quantum defect and 95% due to quantum yield [23]). Volume losses α (for scattering and absorption) in the ceramics were determined by formula

$$\eta_{dif} = \frac{1-R}{1+R}\,\frac{\eta}{\alpha L + 0.5\ln(1/R)}$$

to be $\alpha \leqslant 0.0016$ cm^{-1} at $\eta_{dif} = 70\%$.

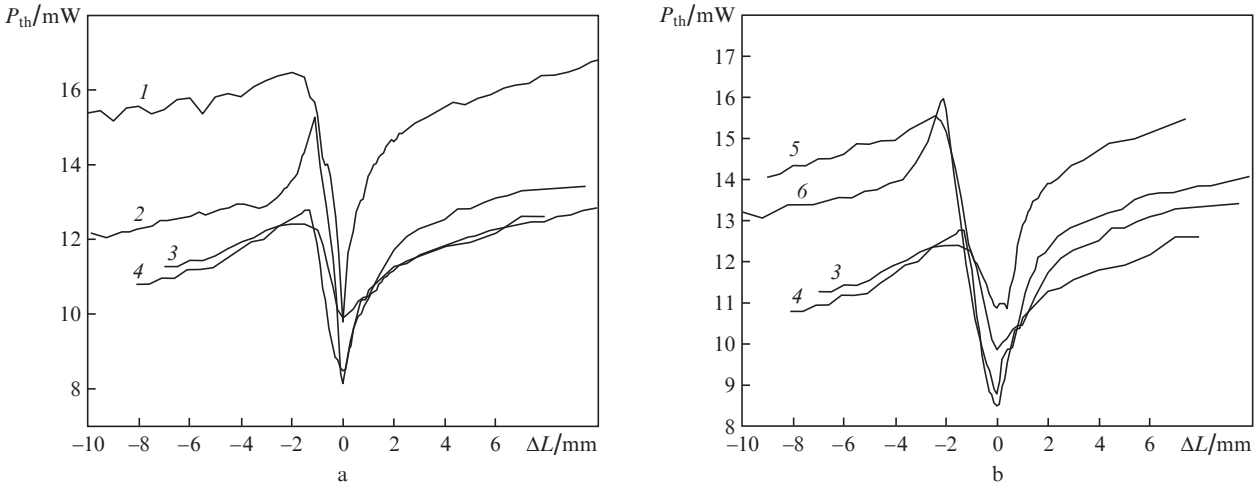

Figure 9. Dependences of lasing thresholds on the deviation from the cavity length in the region of semiconfocal configuration for active ceramic elements (a) (*1*) F, (*2*) K, and (*3*, *4*) R, as well as of (b) ceramic samples R with dimensions of (*4*, *5*, *6*) 3×3×4 and (*3*) 3×3×6 mm cut from different regions of a ceramic disc 70 mm in diameter.

The obtained results allow us to state that the laser ceramics technology created at FIRE corresponds to the world's best level. The technology has been implemented at the SLPG 'Raduga'.

Acknowledgements. This work was supported by the Presidium of the Russian Academy of Sciences (Actual Problems of Photonics, Probing of Inhomogeneous Media and Materials Programme No. 07).

References

1. Esposito L., Costa A.L., Medri V. *J. Europ. Ceram. Soc*., **28**, 1065 (2008).
2. Ikesue A., Furusato A., Kamata K. *J. Am. Ceram. Soc*., **78** (1), 225 (1995).
3. Liu J., Lin L., Li J., Liu J, Yuan Y., Ivanov M., Chen M., Liu B., Ge L., Xie T., Kou H., Shi Y., Pan Y., Guo J. *Ceram. Internat*., **40** (7), 71271 (2014).
4. Li X., Li J.-G., Xiu Z., Huo D., Sun X. *J. Am. Ceram. Soc*., **92** (1), 241 (2009).
5. Patel A.P., Levy M.R., Grimes R.W., Gaume R.M., Feigelson R.S., McClellan K.J., Stanek C.R. *Appl. Phys. Lett*., **93**, 191902 (2008).
6. Boulesteix R., Maitre A., Chretien L., Rabinovitch Y., Salle C. *J. Am. Ceram. Soc*., **96**, 1724 (2013).
7. Kopylov Yu.L., Kravchenko V.B., Bagayev S.N., Shemet V.V., Komarov A.A., Karban O.F., Kaminskii A.A. *Opt. Mater*., **31** (5), 707 (2009).
8. Ge L., Li J., Zhou Z., Liu B., Xie T., Liu J., Kou H., Shi Y., Pan Y., Guo J. *Opt. Mater*., **50**, 25 (2015).
9. Kwadwo A.A., Messing G.L., Dummc J.Q. *Ceram. Internat*., **34** (5), 1313 (2008).
10. Zhang W., Lu T., Ma B., Wei N., Lu Z., Li F., Guan Y., Chen X., Liu W., Qi L. *Opt. Mater*., **35**, 2405 (2013).
11. Stevenson A.J., Li X., Martinez M.A., Anderson J.M., Suchy D.L., Kupp E.R., Dickey E.C., Mueller K.T., Messing G.L. *J. Am. Ceram. Soc*., **94** (5), 1380 (2011).
12. Yagi H., Yanagitani T., Ueda K.-I. *J. Alloys Compd*., **421**, 195 (2006).
13. Yagi H., Yanagitani T., Takaichi K., Ueda K.I., Kaminskii A.A. *Opt. Mater*., **29**, 1258 (2007).
14. Gaume R., Markosyan He.A., Baer R.L. *J. Appl. Phys*., **111**, 093104 (2012).
15. Li Y., Zhou S., Lin H., Hou X., Li W., Teng H., Jia T. *J. Alloys Compd*., **502** (1), 225 (2010).
16. Yang H., Qin X., Zhang J., Ma J., Tang D., Wang S., Zhang Q. *Opt. Mater*., **34** (6), 940 (2012).
17. Kaminskii A.A., Balashov V.V., Cheshev E.A., Kopylov Yu.L., Koromyslov A.L., Krokhin O.N., et al. *Opt. Mater*., **71**, 103 (2017).
18. Bezotosnyi V.V., Cheshev E.A., Gorbunkov M.V., Kostryukov P.V., Tunkin V.G. *Appl. Opt*., **47** (20), 3651 (2008).
19. Lu J., Prabhu M., Ueda K., Yagi H., Yanagitani T., Kudryashov A., Kaminskii A.A. *Laser. Phys*., **11**, 1053 (2001).
20. Boulesteix R., Maitre A., Baumard J.-F., Rabinovitc Y., Reynaud F. *Opt. Express*, **18** (14), 14992 (2010).
21. Bezotosnyi V.V., Cheshev E.A., Gorbunkov M.V., Koromyslov A.L., Kostryukov P.V., Krivonos M.S., et al. *Laser Phys. Lett*., **12**, 025001 (2015).
22. Gorbunkov M.V., Kostryukov P.V., Telegin L.S., Tunkin V.G., Yakovlev D.V. *Quantum Electron*., **37** (2), 173 (2007) [*Kvantovaya Elektron*., **37** (2), 173 (2007)].
23. Vetrovec J. *Proc. SPIE*, **4760**, 491 (2002).